VOID FRACTION MEASUREMENT ON THE LIQUID PISTON IN THE UPWARD VERTICAL AIR-WATER SLUG FLOW

Marco Antonio Sampaio Ferraz de Souza, marco07@fem.unicamp.br
Eugênio Spanó Rosa, erosa@fem.unicamp.br
Universidade Estadual de Campinas – Faculdade de Engenharia Mecânica – Departamento de Energia
Rua Mendeleiev, s/n – Cidade Universitária "Zeferino Vaz"– Caixa Postal 6122 – CEP: 13.083-970 – Campinas - SP

Abstract. *The upward vertical slug flow-pattern in a 26 mm i.d. pipe was studied experimentally using a contact probe to determine the liquid piston local void fraction profile. Experiments were made with water and air in different range of gas and liquid flow rates. The experimentally determined result of the void fraction profiles along the radial and axial directions are presented.*

Keywords: slug flow, void fraction, multiphase flow, contact probe.

1. INTRODUCTION

Slug flow is a gas-liquid flow regime occurring inside pipes over a wide range of gas and liquid flow rates. In vertical flow, this pattern is characterized by the alternance of aerated liquid pistons trailed by elongated gas bubbles, also called Taylor bubbles, which almost fill the pipe cross-section. This type of flow is found in many industrial applications, such as: gas absorption units, nuclear reactors, oil-gas pipelines, steam boilers and heat exchangers. To improve and optimize these industrial processes several studies regarding basic phenomena and slug flow modeling has been done during the past decades. A review on the fundamentals phenomena is given by (Fabre and Liné, 1992). Most of the slug flow models are based on the unit cell concept which considers this flow periodic in time and space. The slug flow properties are estimated using the gas and liquid mass balances along the unit cell and dynamic equation of the liquid surrounding the elongated gas bubble, see Taitel and Barnea (1990). The model is undetermined, it has more unknowns than equations. The solution is obtained by the use of closure equations based on experimental data.

The motivation of this work is the investigation of the gas concentration within the liquid pistons. Even though the major fraction of the gas phase is transported by the elongated gas bubble the aerated liquid piston can transport as much as 20% of the total gas. For referencing purposes, the Fig. 1 shows a sequence of images at intervals of 0.025 s apart in an upward vertical of an air flow with J_G=30 cm/s on a stationary water column. The images show the dispersed air bubbles on the wake of the elongated gas bubble as well as the bubbles which populate the liquid piston.
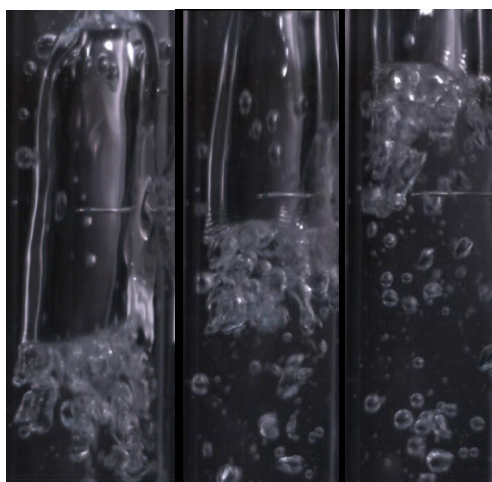

Figure 1. Sequences of images at intervals of 0.025 s apart of an upward vertical air-water slug flow

The gas concentration on the liquid piston is estimated by closure equations mostly based on few experimental measurements which hardly brings universality to the estimates but applies to the experiment where they come from. The uncertainties on the gas concentration estimates propagate to the whole flow model diminishing the model's accuracy. The objective of this work is to perform detailed measurements on the liquid piston void fraction as a form to supply enough data to future development of models or closure laws to predict the liquid piston void fraction.

This work employs a needle contact probe to measure the gas void fraction on the liquid piston and shows the results in terms of void fraction profiles along the radial and axial positions in liquid piston in upward vertical air-water slug flow.

2. EXPERIMENTAL SETUP AND PROCEDURE

An experimental apparatus was assembled to measure the flow properties including the local void fraction in upward vertical air-water intermittent flow in different range of gas and liquid flow rates. A schematic diagram of the experimental flow system is shown in Fig. 2. The test section consists of an acrylic tube of 26 mm attached to a circuit, which contains pumps and compressors which cover a wide range of flows of water and air. The section is divided into two parts: one where the fluids flow separately and the other where they flow mixed characterizing the two-phase flow. The water circuit is composed of a storage tank with capacity of 3 m^3. Water stored in this tank is pumped through a centrifugal pump. The water passes through a Coriolis mass flow meter manufactured by Metroval model RHM15. The air circuit is powered by two compressors in parallel discharging into a storage tank with a capacity of 2 m^3. The air passes through a pressure regulating valve and is directed to a laminar flow element manufactured by Merian model 50 MT10. The two-phase current is formed in a mixer located at the lower end of the line.

The measuring station is positioned at 257D downstream of the mixer. At the station, the passage of liquid pistons and elongated bubbles are monitored by two impedance sensors spaced 112.5 mm apart, and the gas concentration is assessed by a needle contact sensor which is located 330 mm from the upstream impedance sensor. The signals from measuring station are sampled at 3000 Hz during a period of 240 s, digitized and stored in a National Instruments acquisition system.

The mixture leaves the measuring station, travels a distance equivalent to 49D, makes a U turn with a radius of 200 mm on a flexible hose of 37 mm in diameter and then be directed to a vertical tube of 75 mm of diameter. One end of tube is open to the atmosphere while the other end is connected to the water storage tank. This larger diameter vertical tube acts as an air-water separator so that air is freely discharged into the atmosphere while the water is directed to storage tank by gravity. A detailed description of the test circuit is in Gómez (2010).
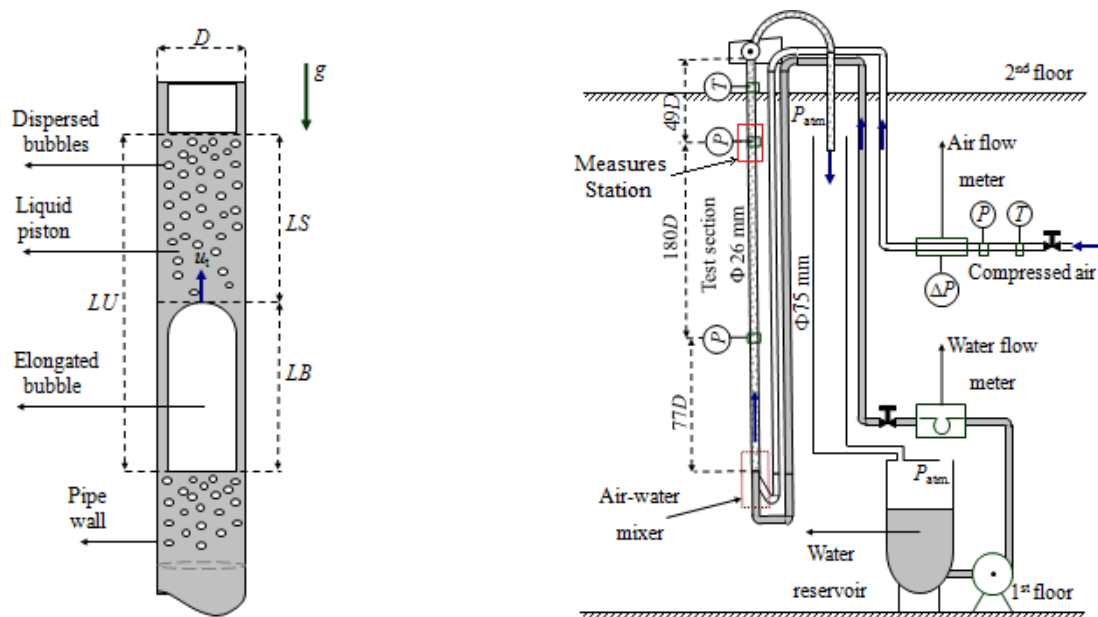

Figure 2. Schematic diagram of a unit and the test section

The slug flow is considered to be formed by similar units which repeat themselves in space and time. A unit consists of an aerated liquid piston trailed by an elongated gas bubble as shown in Fig.2. The test section has the function to acquire and store the signals from the impedance sensors that will identify the velocity of elongated bubble, u_t, the frequency, f, the lengths of the liquid piston, LS, the elongated bubble, LB and unit, LU and the signal from the contact probe will measure the gas concentration in the liquid piston and in the unit.

The liquid and gas superficial velocities, J_L and J_G, ranged from 0.29 to 0.61 m/s and 0.25 to 1.05 m/s, respectively. Superficial velocities are calculated as if the phase was flowing alone in pipe, i.e. $J_k = Q_k/A$, and J is the mixture velocity calculated by $J_L + J_G$. The flow conditions were near atmospheric pressure and the ambient temperature. The data are shown in Tab. 1 and their representation on flow map (Taitel and Barnea, 1980) is in Fig. 3.

Table 1. Liquid and gas volumetric superficial velocities, J_L and J_G

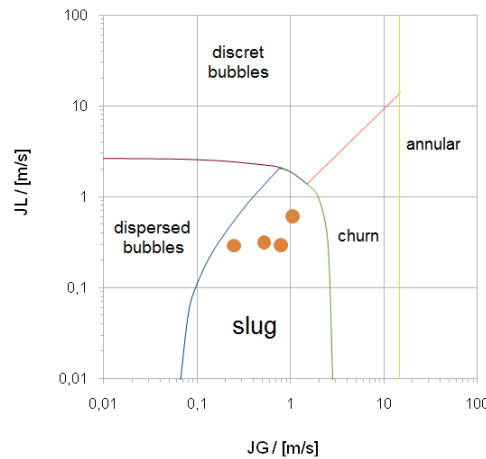| J (cm/s)	J_L (cm/s)	J_G (cm/s)
54	29	25
83	31	52
108	29	78
165	61	105

Figure 3. Flow map and data representation

2.1. The phase indicator function, X_k

The occurrence of a phase k is given by the phase indicator function, X_k. The impedance sensors and contact probe are connected to driver circuit. The output signals are digitized and acquired by a board of National Instruments (NI). Before beginning the two-phase measurements, single-phase liquid and gas measurements were made to calibrate the instrumentation. The signal was calibrated to be in the range of 1 to 5V, where 1V the tube is filled with air and 5V tube filled with water. The magnitude of the voltage signal from the probe is normalized by the ratio

$$V^* = \frac{V - V_{min}}{V_{max} - V_{min}} \tag{1}$$

where V is the instantaneous voltage of the probes, V_{max} and V_{min} are the maximum and minimum voltages observed in the time series of V and V^* is the dimensionless normalized voltage signal. Thus the acquired signal is normalized such that $0 < V^* < 1$, being that $V^* = 0$ corresponds to tube filled with air and $V^* = 1$ corresponds to a tube filled with liquid. Before making the signal processing the program discriminates the occurrence of water and air, and this is done applying a threshold factor, TF, $(0 < TF < 1)$. TF is a logical function that converts the signal of V^* in a square wave, applying the criterion

$$
\begin{aligned}
&\text{If } V^*(t) \geq \text{ TF then } X_k(t) = 1 \ (\text{occurrence of water}) \\
&\text{If } V^*(t) < \text{ TF then } X_k(t) = 0 \ (\text{occurrence of air})
\end{aligned}
\tag{2}
$$

The application of TF allows the identification of the beginning of the bubble and of the beginning of the piston.

2.2 The slug flow properties measurement technique

Figure 4 shows the signal of the twin impedance sensors. In the figure are represented the occurrences of two units for a probe (1). The notation i=1 or 2 refers to the sensor, upstream or downstream, respectively. The index j is the number $(1 \leq j \leq n)$ of the unit. $ts_{i,j}$ is the time duration of the state 1 (piston) in the probe i of the set j (piston/bubble), $tb_{i,j}$ is the duration of the time of the state 0 (bubble) in the probe i of the set j (piston/bubble), $TS_{i,j}$ is the time of the

reference zero (t=0) until the beginning of the piston j in the probe i and $TB_{i,j}$ is the time of the reference zero until the beginning of the bubble j in the probe i.
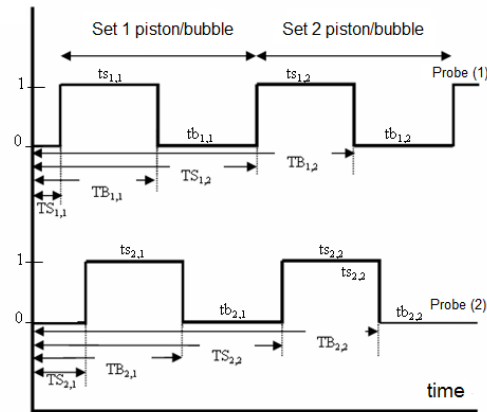

Figure 4. Logic signal idealized to twin sensors spaced S mm. (0) occurrence of gas and (1) occurrence of liquid.

The time spent by the jth bubble to travel the distance separating the twin sensor is

$$\Delta T_{B,j} = TB_{2,j} - TB_{1,j} \tag{3}$$

The bubble nose velocity is

$$u_{tj} = \frac{S}{\Delta t_{B,j}} \tag{4}$$

where S is the spacing between the twin sensors, S=112.5 mm. The length of the jth bubble is calculated by

$$LB_j = u_{tj} \times tb_{1,j} \tag{5}$$

The length of the jth piston is obtained through the relation

$$LS_j = u_{tj} \times ts_{1,j} \tag{6}$$

The frequency of the jth unit is calculated by the expression

$$f_j = \frac{1}{Tu_j} \tag{7}$$

where Tu_j is the time of the all unit, $Tu_{i,j} = ts_{1,j} + tb_{1,j}$.

The algorithm used to process the data identifies each piston and bubble separately. A detailed description of signal processing algorithm is found in Duarte (2007).

2.3. The void fraction measurement technique

The needle contact probe works based on the electrical conductivity between the air and the water. As the needle probe pierces the gas bubbles the conductivity is low and when it is in contact with the water the conductivity is high. The signal resembles a square wave with the high and low output values corresponding to the liquid and gas phase. The local void fraction is measured by taking the ratio between the contact time of the gas phase with the needle and the total acquisition time, Serizawa et al. (1975). The constructive details of the probe are in Guerra and Rosa (2010). Figure 5 shows the probe installed in a 26 mm inner diameter pipe and presents an illustration of the position of the needle in the area section of the pipe.

Figure 5. Position of the needle in the area section of pipe

With the aid of a micrometer the probe was displaced at 10 different radial positions (see Tab. 2) to get the void fraction distribution. The micrometer was zeroed on the inner wall opposite to the probe and it sweep across 13 mm the inner wall to the pipe center. The acquisition was made in 240 seconds with a frequency of 3000 Hz and the signal was analyzed in LabView environment. Figure 6 presents the signal of three liquid pistons acquired by the contact probe superposed by the square wave generated by applying a TF 0.8. The next step was to develop a module in the LabView environment to determine the average void fraction of the unit and of the liquid piston. Analyzing the nature of voltage signals, a signal processing scheme is developed for measurements of time-averaged void fractions.

Table 2. Different radial positions of the needle.

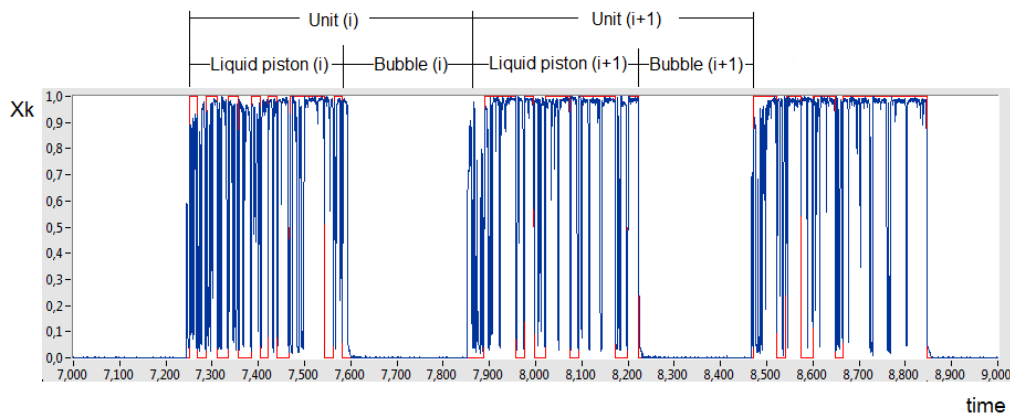| Position	r/R	R (mm)
1	0.95	12.35
2	0.90	11.70
3	0.85	11.05
4	0.80	10.40
5	0.70	9.10
6	0.60	7.80
7	0.50	6.50
8	0.30	3.90
9	0.10	1.30
10	0	0

Figure 6. Typical contact probe output signal of three liquid pistons

To process the contact probe voltage signal output for calculating the time-averaged void fraction, the gas and liquid phases must be distinguished from each other and phase signals must be separated.

3. SIGNAL PROCESSING

The void fraction at any radial position is a ratio between the air residence time and the sampling time. Since the signal is given in discrete form (Fig. 7), the void fraction in any position, r/R can be written as

$$\alpha\left(\frac{r}{R}\right) = \frac{1}{tt}\sum_{i=1}^{N} t'_i = \frac{1}{N}\sum_{i=1}^{N} X_{ki} \tag{8}$$

where t'_i is time that each bubble remains in contact with the probe, tt is the total sampling time and N is the number of points in the sample. The hypothesis of the time-average process is guaranteed provided that the time-scale of the flow is sufficiently greater than the sampling interval, tt.
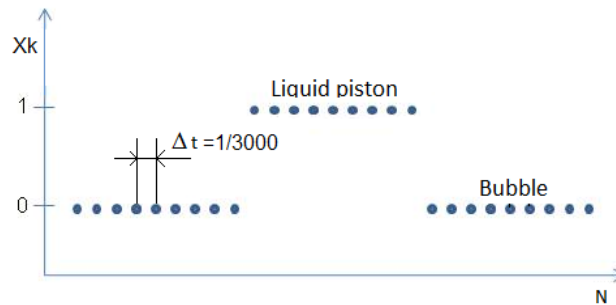

Figure 7. Signal discrete form

3.1 Void fraction of the unit, α_u

Equation (8) samples the gas occurrence of the dispersed bubbles and of the elongated bubbles in a continuous slug. If one considers that the flow has an average liquid piston and an average elongated gas bubble, the resultant void fraction value represents, at a given radial position, the unit cell void fraction. If one integrates α along the radial direction one gets the unit averaged void fraction defined as

$$< \alpha_u > \ = \frac{1}{A}\int \alpha\left(\frac{r}{R}\right) 2\pi r dr \tag{9}$$

Equation (9) is an average that condenses the radial direction and the time by a single value α_u.

3.2 Void fraction in the liquid slug, α_s

The ensemble average of X_k for each position (r/R) and (z/D) will provide the average void fraction, $\alpha(r/R, z/D)$. As each liquid piston has different lengths and times is necessary to interpolate X_k which is determined at discrete points. Initially the time interval is converted to a spatial dependence in the z direction, multiplying the duration of each liquid piston by its respective velocity of the bubble, u_t as shown in Fig. 8.
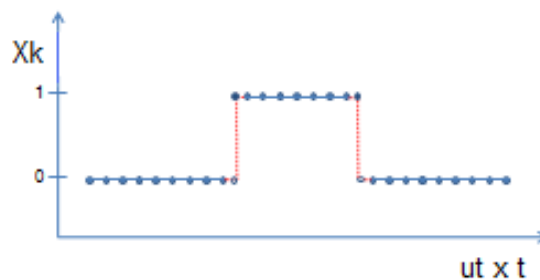

Figure 8. Signal of the contact probe into the liquid piston as a spatial function

The next step is to extract from each signal taken at a specific radial position the phase indicator function X_k corresponding to each individual liquid piston intercepted by the probe. The procedure is repeated for different radial positions and constituted the ensemble of X_k for the distinct liquid pistons taken at distinct radial positions, see representation in Fig. 9.
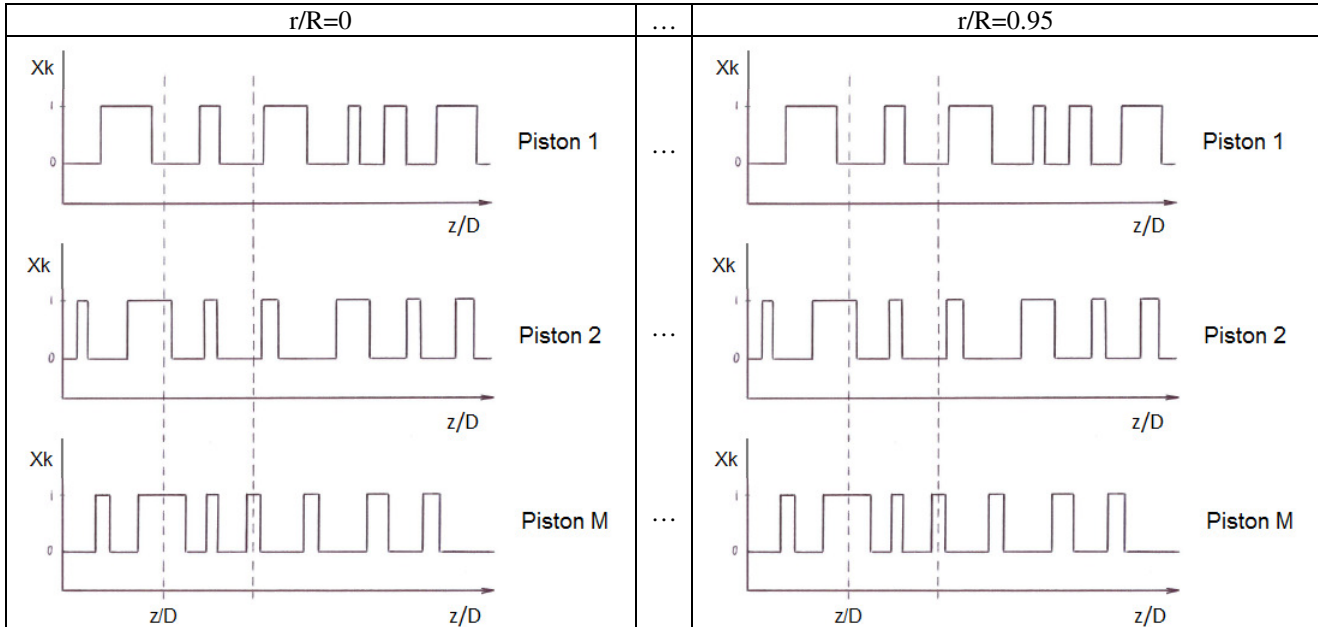

Figure 9. Void fraction of each liquid piston in each radial position

The average void fraction of all liquid pistons in a given radial position (r/R) is the sum of the X_k in each axial position (z/D) of each liquid piston divided by the number of liquid piston.

$$\alpha_S\left(\frac{r}{R},\frac{z}{D}\right) = \frac{\sum_{i=1}^{M} X_{ki}\left(\frac{r}{R},\frac{z}{D}\right)}{M} \qquad (10)$$

where M is the number of liquid pistons. The average length of all liquid pistons is calculated as the arithmetic mean of pistons length plus one standard deviation.

4. EXPERIMENTAL RESULTS AND DISCUSSIONS

4.1 Radial profiles of the unit void fraction

The radial void fraction distribution of the unit, α_u are shown in Fig. 10 for different J_L and J_G values. The void fraction distribution shows a decrease near the tube wall indicating the existence of a liquid layer with low voids. Far from the wall r/R<0.8 the profile is nearly flat. Keeping constant J_L and increasing J_G the profiles are shifted upward. Also for points with the same air to water ratio, i.e. J_L and J_G of 31-52 and 61-105 the profiles are almost coincident.
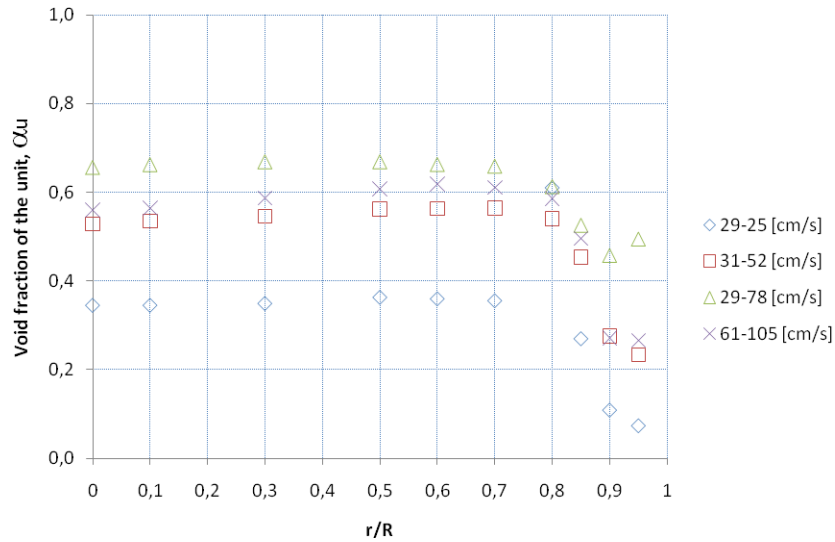
Figure 10. Radial profiles of the average void fraction of the unit

4.2 Spatial distribution of the average void fraction in the liquid piston

The spatial distribution of the void fraction in liquid piston is shown in Fig. 11. The surface show the void fraction in the liquid piston for liquid superficial velocity, $J_L = 0.29$ m/s and gas superficial velocity, $J_G = 0.51$ m/s.

The position z/D represents the head of the liquid piston or the tail of the gas bubble. It is observed a sharp decrease in void fraction near z/D=3 and then an increase.
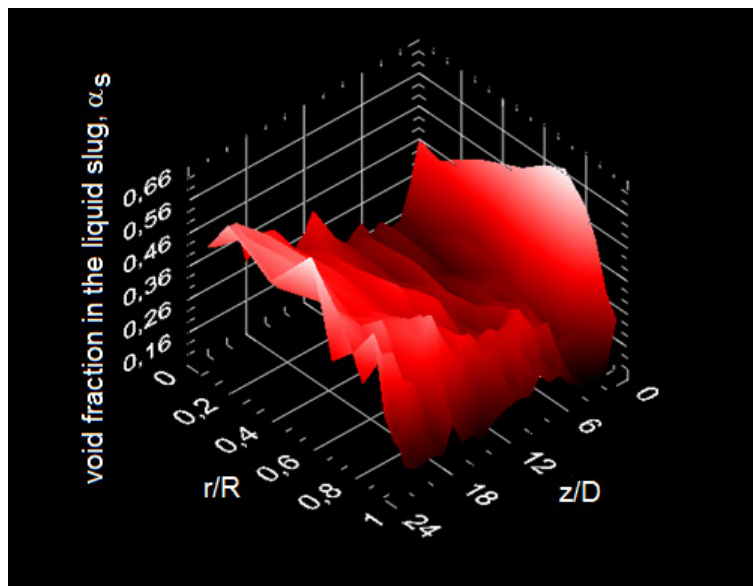

Figure 11. Spatial distribution of the average void fraction in the liquid piston

4.3 Liquid piston void fraction: radial profiles

The void fraction changes along the axial length of the liquid piston are condensed to a single radial position by averaging. Scanning at different radial positions it is possible evaluate the liquid piston void fraction radial profile as shown in Fig. 12. It is observed that near the wall the void fraction is low, as expected. The profile peaks at nearly r/R ~ 0.8 and then exhibits a mild decrease towards the pipe's center line. The measured profile has similarity with experimental data taken for bubbly flow including the wall peaking phenomenon (Serizawa 1986) but the void fraction values at the pipe core are far superior. The differences on the values are in part because the liquid slugs may attain averaged void fractions, as high as 0.26. These high values are due the detachment of air bubbles caused by downward liquid film stream impinging into the upward liquid piston. Keeping constant the liquid flow and increasing the gas flow

displaces the void profiles upward; also fixing the same air to water ratio the resultant profiles are similar likewise observed in Fig. 10.
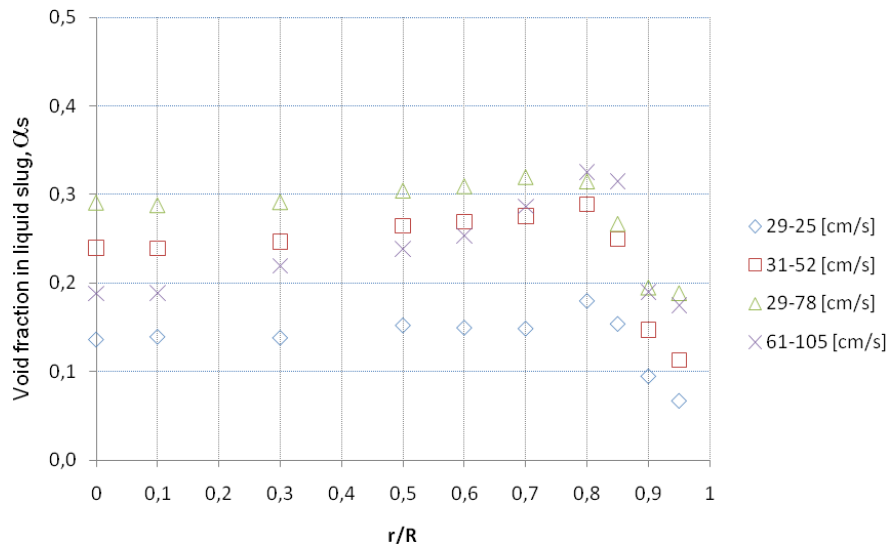

Figure 12. Radial profiles of the average void fraction in liquid piston

4.4 Axial profiles of the void fraction in the liquid slug

The void fraction changes along the radial direction of the liquid piston are condensed to a single axial position by averaging. Scanning at different axial positions it is possible evaluate the liquid piston void fraction axial profile as shown in Fig. 13. The profiles show a sharp decrease attaining a minimum at $Z/D \approx 3$ and then a mild increase. The sharp decrease is mainly attributed to the existing recirculation zone at the tail of the elongated gas bubble. This zone is highly aerated and the bubble population inside this zone keeps in a cycle of detaching and attaching at the elongated gas bubble tail. The mild increase in the void fraction for $Z/D > 3$ is attributed to a relative deceleration of the liquid in regard to the dispersed bubbles but this phenomena has to be further investigated.
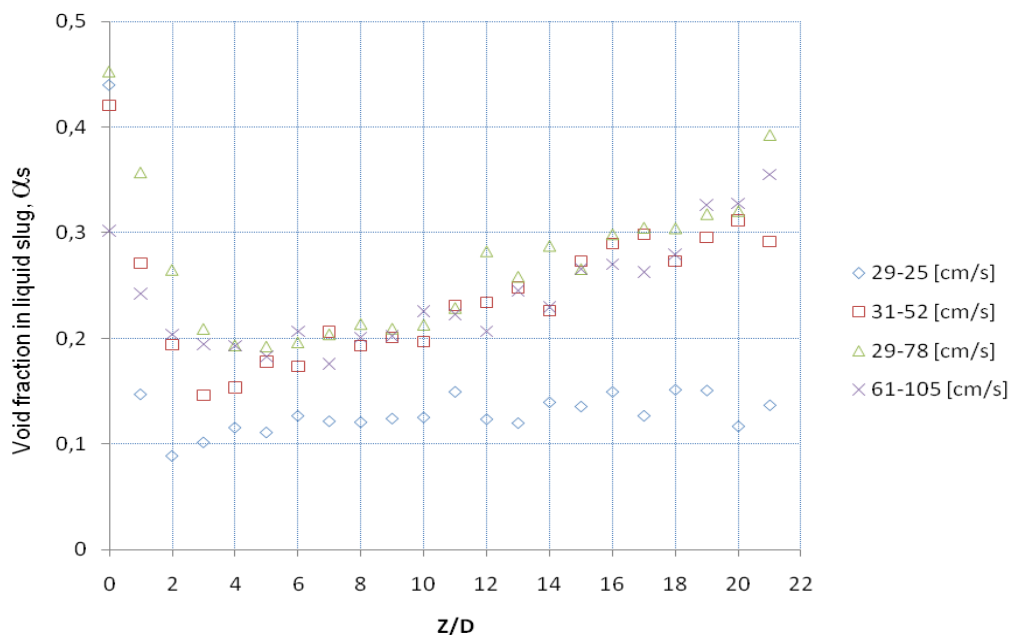

Figure 13. Axial profiles of the average void fraction in liquid slug

4.5 Averaged experimental measurements

Table 3 summarizes the experimental measurements obtained for the liquid and gas superficial velocities and for the translation velocity of the bubble, for the length of the elongated bubble, liquid piston and unit and for the average void fraction of unit and liquid piston.

Table 3. Summary of the experimental measurements.

(cm/s)	(cm/s)	(cm/s)	(cm/s)	(L/D)	(L/D)	(L/D)	(---)	(---)
J	J_L	J_G	u_t	LB	LS	LU	α_u	α_s
54	29	25	71	6	15	22	0.31	0.13
83	31	52	110	14	16	29	0.46	0.22
108	29	78	150	27	17	43	0.57	0.26
165	61	105	216	23	17	39	0.50	0.23

5. CONCLUSIONS

It is demonstrated that the electrical resistivity probe technique can be successfully utilized in a vertical two-phase slug flow-pattern to distinguish the gas and liquid phases and to measure the time-averaged local void fractions of the dispersed bubbles in the liquid pistons and in the unit. The experimental results for a 26 mm i.d. upward vertical slug flow indicate that the liquid piston void fraction profiles are nearly flat along the radial direction and exhibits a sharp drop near the wall and the axial direction they show a mild increase. The results obtained for the void fraction distribution in the liquid piston showed physical phenomena that occur in this type of flow as the increase of the gas concentration in front of the liquid piston due to the removal of small bubbles from trail of the elongated bubble at the moment in which the liquid passes from the film to the next piston forming dispersed bubbles.

6. REFERENCES

Duarte, M., 2007, "Influência da viscosidade sobre o escoamento gás-líquido intermitente". Dissertação de Mestrado, Unicamp.

Fabre, J. Liné, A., 1992, "Modeling of two-phase slug flow". Annual Review of Fluid Mechanics 24, 21-46.

Gómez, L. G., 2010, "Estudo experimental de escoamentos líquido-gás intermitentes em tubulações inclinadas". Dissertação de Mestrado, Unicamp.

Guerra, R, F., Rosa, E, S., 2010, "Projeto e construção de uma Sonda Elétrica". Projeto de Iniciação Científica, Unicamp.

Serizawa, A., Kataoka, I., Michiyoshi, L., 1975, "Turbulence structure of air-water bubbly flow. I. Measuring techniques, Int. J. Multiphase Flow 2 , 221-233.

Taitel, Y., Barnea, D., Dukler, A., 1980, "Modelling flow pattern transitions for steady upward gás-liquid flow in vertical tubes". AIChE J. 3, 345-354.

Taitel, Y., Barnea, D., 1990, "Two-phase slug flow". Adv. Heat Transfer 20, 43-132.

7. RESPONSIBILITY NOTICE

The authors are the only responsible for the printed material included in this paper.